DTP/94/10
June 1994

Anomalous quartic couplings in $W^+W^-\gamma$ production at e^+e^- colliders

Ghadir Abu Leil

and

W.J. Stirling

Department of Physics, University of Durham
Durham DH1 3LE, England

Abstract

We study the process $e^+e^- \to W^+W^-\gamma$ at high-energy e^+e^- colliders to investigate the effect of genuine quartic $W^+W^-\gamma\gamma$ and $W^+W^-Z\gamma$ anomalous couplings on the cross section. Deviations from the Standard Model predictions are quantified. We show how bounds on the anomalous couplings can be improved by choosing specific initial state helicity combinations. The dependence of the anomalous contributions on the collider energy is studied.

1 Introduction

In the Standard Model (SM) of electroweak interactions, the $\mathrm{SU}_L(2)\times\ \mathrm{U}_Y(1)$ non-abelian nature of the gauge symmetry relates the trilinear and quadrilinear vertices to the universal SU(2) gauge coupling, g_w. At tree level there are only two trilinear vertices, $W^+W^-\gamma$ and W^+W^-Z, and four quartic vertices $W^+W^-\gamma\gamma$, $W^+W^-\gamma Z$, W^+W^-ZZ and $W^+W^-W^+W^-$. Only recently have experiments begun to test these vertices directly. At the CERN and FNAL $p\bar{p}$ colliders, a handful of $W^\pm\gamma$ events have been used to place limits on the anomalous $W^+W^-\gamma$ and W^+W^-Z trilinear couplings [1, 2, 3]. The LEP II e^+e^- collider will also test the trilinear vertices through the total W^+W^- cross section [4]. However, independent tests of the *quartic* couplings require more complicated processes. One of the most accessible in the short term is the process $e^+e^-\to W^+W^-\gamma$, and it is this which provides the focus of the present study.

Studying the gauge boson interactions (of the W boson in particular) will help our understanding of the mechanism of spontaneous symmetry breaking. Since the gauge-boson self interaction originates in the non-abelian kinetic term of the Lagrangian, it is directly related to the Goldstone modes and the Higgs particle. The quartic couplings in particular will provide a way of testing the Higgs mechanism, either verifying the local gauge invariance or signaling the existence of new physics beyond the Standard Model. A review of the importance of quartic couplings in probing new physics can be found in Ref. [5].

There is an important distinction between anomalous trilinear and genuine anomalous quartic couplings, *i.e.* those which give no contribution to the trilinear vertices [6]. Whereas the trilinear couplings involving W's are essentially form factors where massive fields are integrated out at the one-loop level, the anomalous quartic couplings are contact interactions – manifestations of the exchange of heavy particles. One can therefore imagine a theory in which the trilinear couplings have their Standard Model values, but the quartic couplings are modified by any number of independent anomalous contact interactions.

In this paper we study the effect of anomalous quartic couplings in the process $e^+e^-\to W^+W^-\gamma$ at high energy. Our work builds on and extends the analysis of [5, 6], in that we investigate the collider energy and polarization dependence of the anomalous effects. In Section 2 we discuss the contributions of the anomalous operators in the context of $W^+W^-\gamma$ production and in Section 3 the numerical results are presented.

2 The interaction Lagrangian

In this section we discuss the lowest dimension operators which lead to genuine quartic couplings. These operators must of course have the proper Lorentz structure, and should also respect the custodial SU(2) symmetry in order to evade experimental bounds on the ρ parameter [7]. The phenomenological Lagrangian should also respect the full U(1) gauge invariance, as at least one of the fields is a photon. For simplicity, we restrict the study to C- and P-conserving operators. The lowest dimension operators that satisfy the above constraints are of dimension 6, since the $\mathrm{U}(1)_{em}$ symmetry requires derivatives [6]. These operators[1] are:

$$\mathcal{L}^0 = -\frac{\pi\alpha}{4\Lambda^2} a_0 F_{\alpha\beta} F^{\alpha\beta} (\vec{W}_\mu \cdot \vec{W}^\mu) \tag{1}$$

$$\mathcal{L}^c = -\frac{\pi\alpha}{4\Lambda^2} a_c F_{\alpha\mu} F^{\alpha\nu} (\vec{W}^\mu \cdot \vec{W}_\nu) \tag{2}$$

$$\mathcal{L}^n = i\frac{\pi\alpha}{4\Lambda^2} a_n \epsilon_{ijk} W^{(i)}_{\mu\alpha} W^{(j)}_{\nu} W^{(k)\alpha} F^{\mu\nu} \tag{3}$$

where $\vec{W}_\mu$ is an SU(2) triplet, and $F^{\mu\nu}$ and $\vec{W}^{\mu\nu}$ are the $\mathrm{U}(1)_{em}$ and the SU(2) field strengths respectively. The parameter Λ is an unknown 'new-physics' scale which, following convention, we take to be M_W.

The physical Lagrangians are obtained when the above are written in terms of the physical fields W^+, W^- and $Z^0 = W^3 \cos\theta_w$. The physical basis for $\mathcal{L}^0$ and $\mathcal{L}^c$ is obtained by the substitution [6]

$$\vec{W}_\mu \cdot \vec{W}_\nu \rightarrow \; 2W^+_\mu W^-_\nu + \frac{1}{\cos\theta^2_w} Z_\mu Z_\nu \tag{4}$$

while the physical basis for the part of $\mathcal{L}^n$ which gives rise to quartic couplings is

$$\begin{aligned} \vec{W}_{\mu\alpha} \cdot (\vec{W}_\nu \times \vec{W}^\alpha) \;\rightarrow\; & \frac{i}{\cos\theta_w} \Big[(\partial_\mu W^+_\alpha - \partial_\alpha W^+_\mu)(Z_\nu W^{-\alpha} - Z^\alpha W^-_\nu) \\ & + (\partial_\mu W^-_\alpha - \partial_\alpha W^-_\mu)(Z^\alpha W^+_\nu - Z_\nu W^{\alpha+}) \\ & + (\partial_\mu Z_\alpha - \partial_\alpha Z_\mu)(W^-_\nu W^{+\alpha} - W^+_\nu W^{-\alpha}) \Big] \end{aligned} \tag{5}$$

The effective Lagrangians $\mathcal{L}^0$ and $\mathcal{L}^c$ give rise to an anomalous $W^+W^-\gamma\gamma$ coupling, whereas $\mathcal{L}^n$ gives rise to an anomalous $W^+W^-Z\gamma$ coupling. The corresponding Feynman rules are listed in Ref. [7].

[1] Note that the operator $\mathcal{L}^0$ can be parametrized by the exchange of a neutral scalar particle.

3 Numerical results and conclusions

We begin this section by analysing the effect of the anomalous couplings a_0, a_c and a_n on the total $W^+W^-\gamma$ production cross section at a 500 GeV e^+e^- collider [5]. The anomalous cross sections are quadratic functions of the parameters a_0, a_c and a_n. Fig. 1 shows the total cross-sections with one parameter being different from zero at any one time. In order to avoid collinear singularities caused by the massless photon the following rapidity and energy cuts are implemented

$$|\eta_\gamma| \leq 2 \,, \qquad E_\gamma \geq 20 \text{ GeV} \tag{6}$$

In addition, all the initial and final particles are separated by at least 15°. Other parameter values are $M_W = 80$ GeV/c^2, $\sin^2\theta_W = 0.23$ and $\Gamma_Z = 2.55$ GeV. With these parameters, the Standard Model total cross section ($a_0 = a_c = a_n = 0$) is 123.4 fb, which corresponds to a total of $N(W^+W^-\gamma) = 1234$ events for an integrated luminosity of $\mathcal{L} = 10$ fb^{-1}. The two horizontal lines in Fig. 1 correspond to a $\pm 3\sigma$ statistical variation of the Standard Model result, *i.e.*

$$\delta\sigma_{SM} = \pm 3 \sqrt{\frac{\sigma_{SM}}{\mathcal{L}}} \tag{7}$$

where the integrated luminosity is again taken to be $\mathcal{L} = 10$ fb^{-1}. The $\pm 3\sigma$ band corresponds to the following variation in the anomalous couplings:

$$\begin{aligned} -0.64 \leq \;& a_0 \;& \leq 0.42 \\ -1.38 \leq \;& a_c \;& \leq 0.65 \\ -3.9 \leq \;& a_n \;& \leq 4.25 \,, \end{aligned} \tag{8}$$

indicating that the sensitivity is greatest for the a_0 parameter and least for the a_n parameter.

We next investigate the dependence of the cross sections on the photon energy. Fig. 2 shows the E_γ distribution at $\sqrt{s} = 500$ GeV, with the same cuts and parameters as before. Fig. 2(a) shows the distributions for $a_0 = 0$ (Standard Model, solid line), $a_0 = \pm 1$ (dashed lines) and $a_0 = 0.42$ (the 3σ value, dotted line), the other anomalous couplings being set to zero. Evidently the bulk of the sensitivity comes from the hard photon end of the spectrum. This is not unexpected, since the additional contributions do not give rise to infra-red singularities as $E_\gamma \to 0$. Similar remarks apply to the other parameters. Figs. 2(b) and (c) show the effect on the photon energy distribution of varying a_c and a_n respectively.

To try and improve the sensitivity to the anomalous couplings, we consider next the helicity decomposition of the cross section. The amplitude for $e^+e^- \to W^+W^-$ contains two different types of contribution: s-channel Z, γ exchange and t-channel

neutrino exchange. The anomalous quartic coupling contributions to $W^+W^-\gamma$ production, however, only receive contributions from the former, *i.e.* $e^+e^- \to Z^*, \gamma^* \to W^+W^-\gamma$. It follows that the effects will be largest in the *positive helicity* initial-state configuration, $\lambda_{e^-}\lambda_{e^+} = +1$, since this receives no contribution from the 'Standard Model background' neutrino-exchange diagrams. Fig. 3 shows the distribution $d\sigma^{\pm}(a_i)/dE_\gamma$ $(i = 0, c)$ at 500 GeV for (a) the positive helicity $\lambda_{e^-}\lambda_{e^+} = +1$ cross section (σ^+) and (b) the negative helicity $\lambda_{e^-}\lambda_{e^+} = -1$ cross section (σ^-). For the same variation in the a_i, the effect is indeed much larger in the former.

Unfortunately, at these energies the positive helicity cross section is in absolute terms much smaller than the negative helicity cross section. This is illustrated in Fig. 4, which shows the spin decomposition of the total $W^+W^-\gamma$ Standard Model cross section as a function of $E_{\rm beam}$. There is a difference of some two orders of magnitude between σ^- and σ^+.

Finally, we address the question of whether there is any possibility of seeing an effect in $W^+W^-\gamma$ production at lower e^+e^- collider energies. We consider variations in a_0 only – similar remarks apply to the other couplings. The problem at lower energies is that phase space restricts the photon to be soft, which is where the sensitivity to the anomalous couplings is least. This is illustrated in Fig. 5, which shows the ratio of σ, σ^+ and σ^- for $a_0 = 1$ to that of the corresponding Standard Model cross section, as a function of $E_{\rm beam}$, with the same photon cuts as before. Below $E_{\rm beam} = 150$ GeV the effects are negligible. The increased sensitivity to a_0 in σ^+ is partially offset by the much smaller cross section in this channel. Taking $\mathcal{L} = 10$ fb^{-1} for both the positive and negative helicity channels, we calculate from Fig. 5 that at 500 GeV, $a_0 = 1$ gives a 7.5σ increase of σ^- and a 47σ increase of σ^+. The corresponding numbers for 300 GeV collisions are 0.4σ and 1.0σ respectively.

Of course we do expect to obtain a handful of $W^+W^-\gamma$ events even at LEP II, and from these it will be possible to derive very crude limits on the anomalous quartic couplings. Fig. 6 shows the total $W^+W^-\gamma$ cross sections for $E_\gamma > 20$ GeV, $|\eta_\gamma| < 2$ photons in e^+e^- collisions at 200 GeV, as a function of a_0 and a_c.[2] Again, the dependence is quadratic. Note the vastly expanded horizontal scale compared to Fig. 1.

In conclusion, quartic couplings can provide a window on new physics beyond the Standard Model. We have quantified the effect of various types of anomalous operators on the $W^+W^-\gamma$ production cross section in e^+e^- collisions. The effects are largest in the positive helicity cross section, although this represents only a small fraction of the total cross section. This type of physics is best suited to high energy colliders – there is an enormous increase in sensitivity in going from $\sqrt{s} = 300$ GeV to $\sqrt{s} = 500$ GeV – although some crude limits should be possible even from a handful of events at LEP II.

[2] the dependence on a_n is negligible at this energy

Acknowledgments

This work was supported in part by an ICSC World Laboratory Studentship and a University of Durham Research Studentship.

References

[1] UA2 collaboration: J. Alitti *et al.*, Phys. Lett. **B277** (1992) 194.

[2] CDF collaboration: presented by M. Lindgren at the International Symposium on "Physics Doesn't Stop: Recent Developments in Phenomenology", University of Wisconsin, Madison, April (1994).

[3] D0 collaboration: presented by S. Lami at the International Symposium on "Physics Doesn't Stop: Recent Developments in Phenomenology", University of Wisconsin, Madison, April (1994).

[4] M. Davier *et al.*, Proc. ECFA Workshop on LEP 200, Aachen, Germany (1986), eds. A. Böhm and W. Hoogland, report CERN 87-08 (1987) , Vol.I, p.120.

[5] G. Bélanger and F. Boudjema, in Proc. Workshop on "e^+e^- Collisions at 500 GeV: the Physics Potential", Munich, Annecy, Hamburg (1991), ed. P.M. Zerwas, report DESY 92-123B (1992) p.763.

[6] G. Bélanger and F. Boudjema, Phys. Lett. **B288** (1992) 201.

[7] O.J.P. Eboli, M.C. Gonzalez-Garcia and S.F. Novaes, Nucl. Phys. **B411** (1994) 381.

Figure Captions

[1] The total cross section for the process $e^+e^- \to W^+W^-\gamma$ at $\sqrt{s} = 500$ GeV as a function of the anomalous couplings a_0, a_c and a_n. The $\pm 3\sigma$ variation about the SM cross-section is indicated by the horizontal lines.

[2] The photon energy distribution $d\sigma/dE_\gamma$ for different values of (a) the a_0 parameter, (b) the a_c parameter, and (c) the a_n parameter, at $\sqrt{s} = 500$ GeV.

[3] The (a) positive-helicity and (b) negative-helicity cross sections $d\sigma^{\pm}(a_i)/dE_\gamma$ as a function of the photon energy, at $\sqrt{s} = 500$ GeV.

[4] The positive- and negative-helicity contributions to the Standard Model $e^+e^- \to W^+W^-\gamma$ cross section as a function of the beam energy.

[5] The ratio of the total, negative-helicity and positive-helicity cross sections for $a_0 = 1$ to those of the Standard Model ($a_0 = 0$), as a function of the beam energy.

[6] The dependence of the total $e^+e^- \to W^+W^-\gamma$ cross section on the anomalous couplings a_0 and a_c at LEP II ($\sqrt{s} = 200$ GeV).

This figure "fig1-1.png" is available in "png" format from:

http://arXiv.org/ps/hep-ph/9406317v1

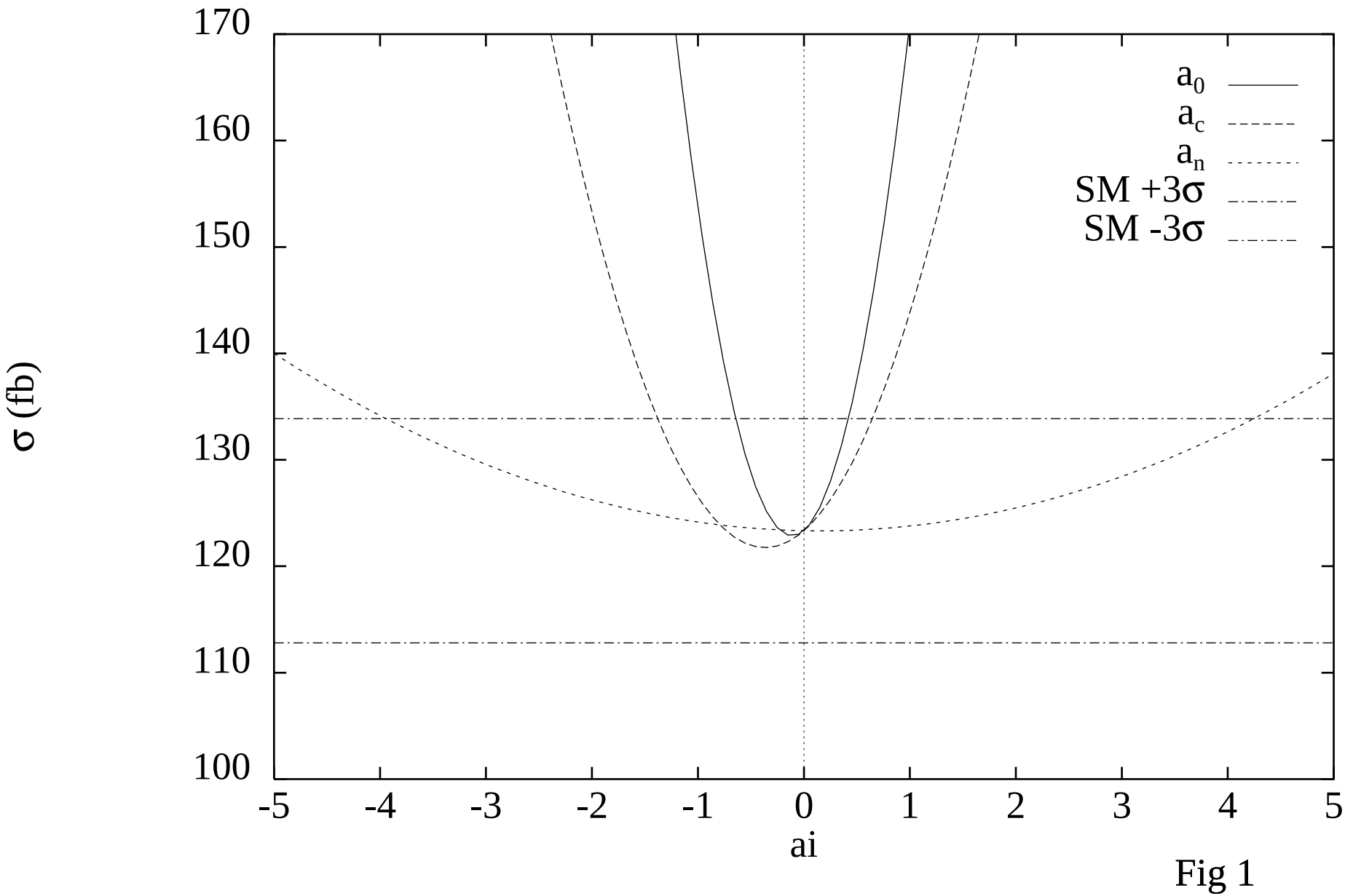
170
160
150
140
130
120
110
100
σ (fb)
-5
-4
-3
-2
-1
0
1
2
3
4
5
ai
a0
ac
an
SM +3σ
SM -3σ

Fig 1

This figure "fig2-1.png" is available in "png" format from:

http://arXiv.org/ps/hep-ph/9406317v1

This figure "fig1-2.png" is available in "png" format from:

http://arXiv.org/ps/hep-ph/9406317v1

This figure "fig2-2.png" is available in "png" format from:

http://arXiv.org/ps/hep-ph/9406317v1

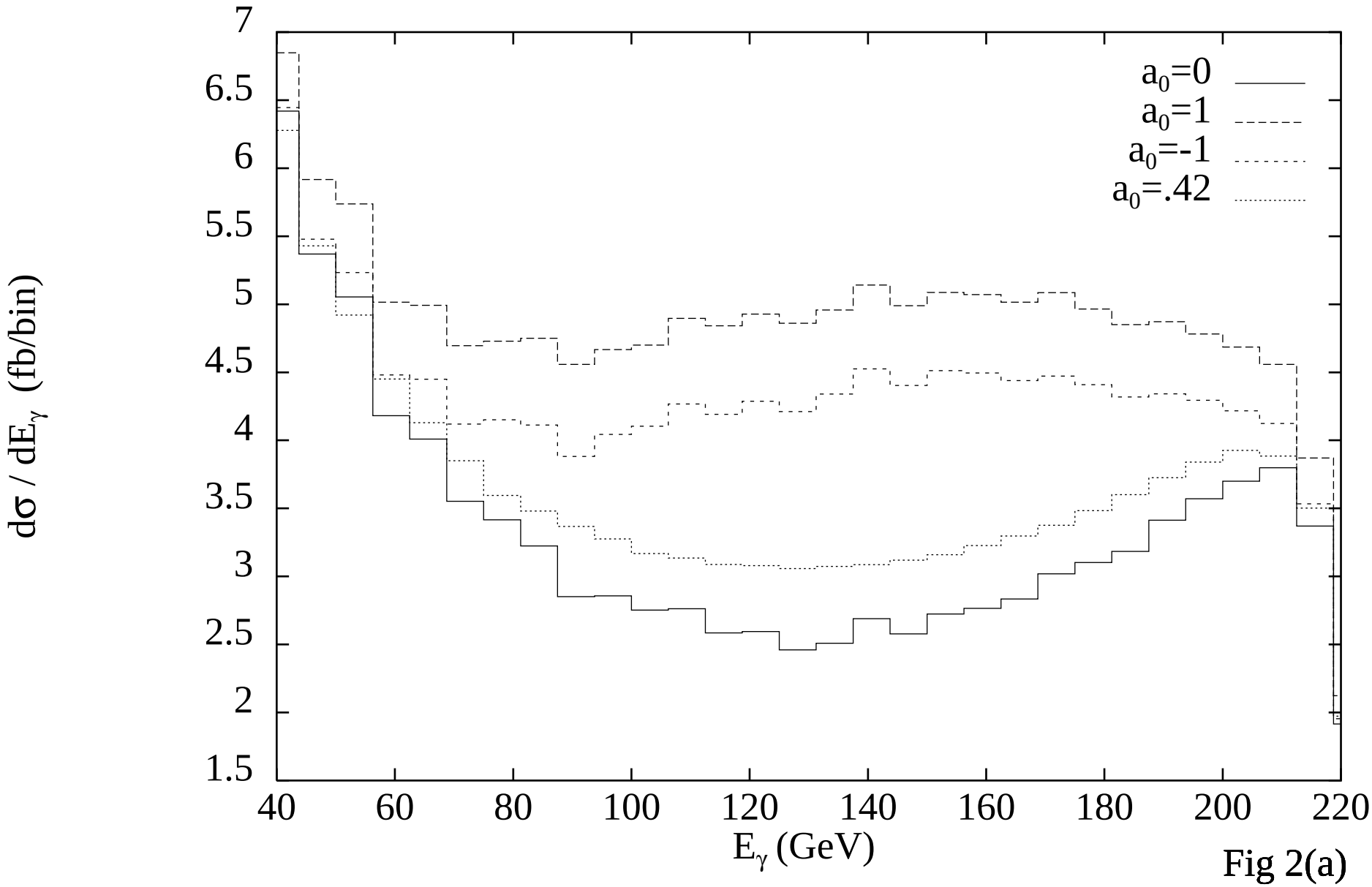
7
6.5
6
5.5
5
4.5
4
3.5
3
2.5
2
1.5
40
60
80
100
120
140
160
180
200
220
$d\sigma / dE_\gamma$ (fb/bin)
E_γ (GeV)
a_0=0
a_0=1
a_0=-1
a_0=.42

Fig 2(a)

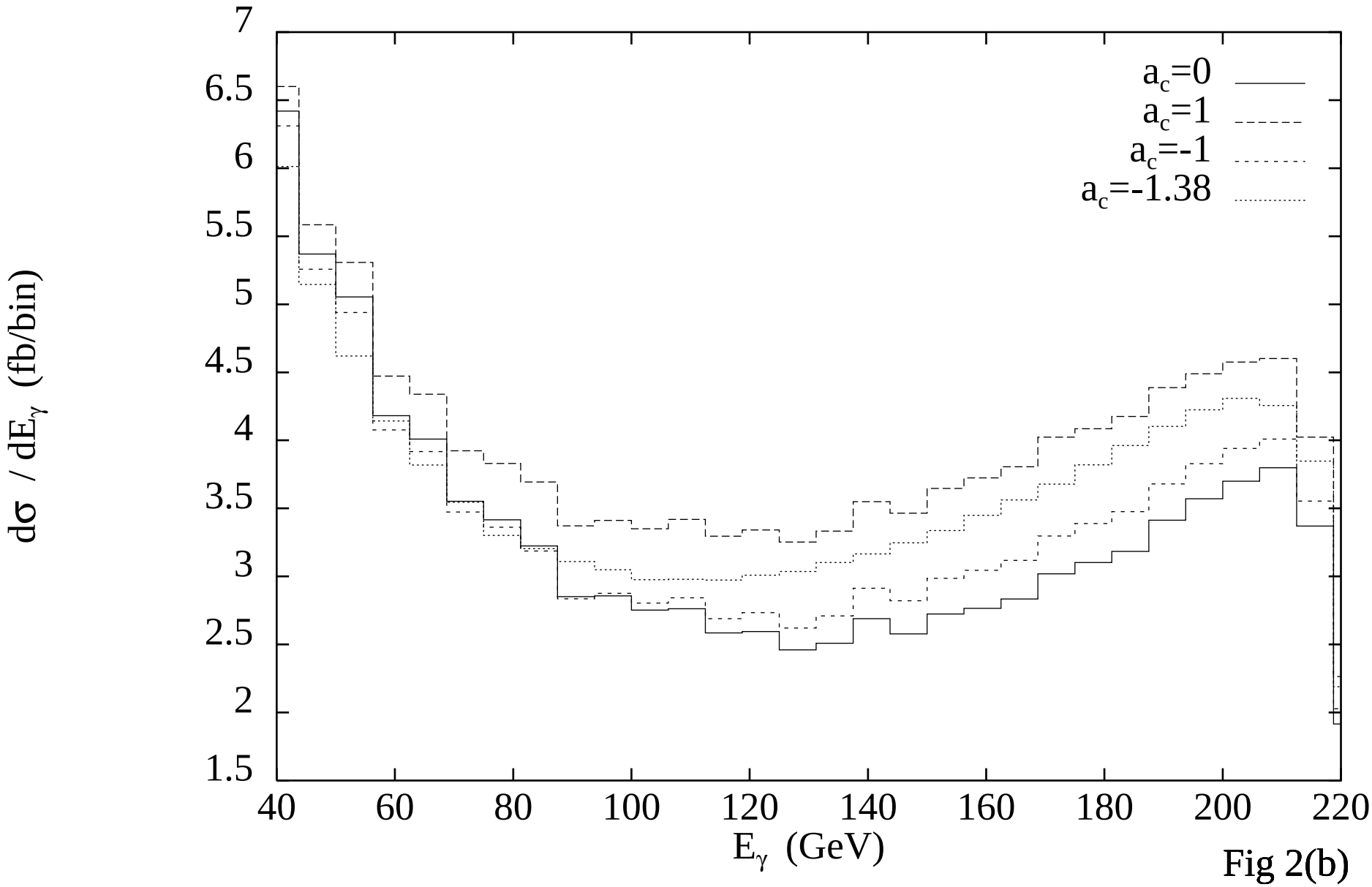
7
6.5
6
5.5
5
4.5
4
3.5
3
2.5
2
1.5
40
60
80
100
120
140
160
180
200
220
a_c=0
a_c=1
a_c=-1
a_c=-1.38
$d\sigma / dE_\gamma$ (fb/bin)
E_γ (GeV)

Fig 2(b)

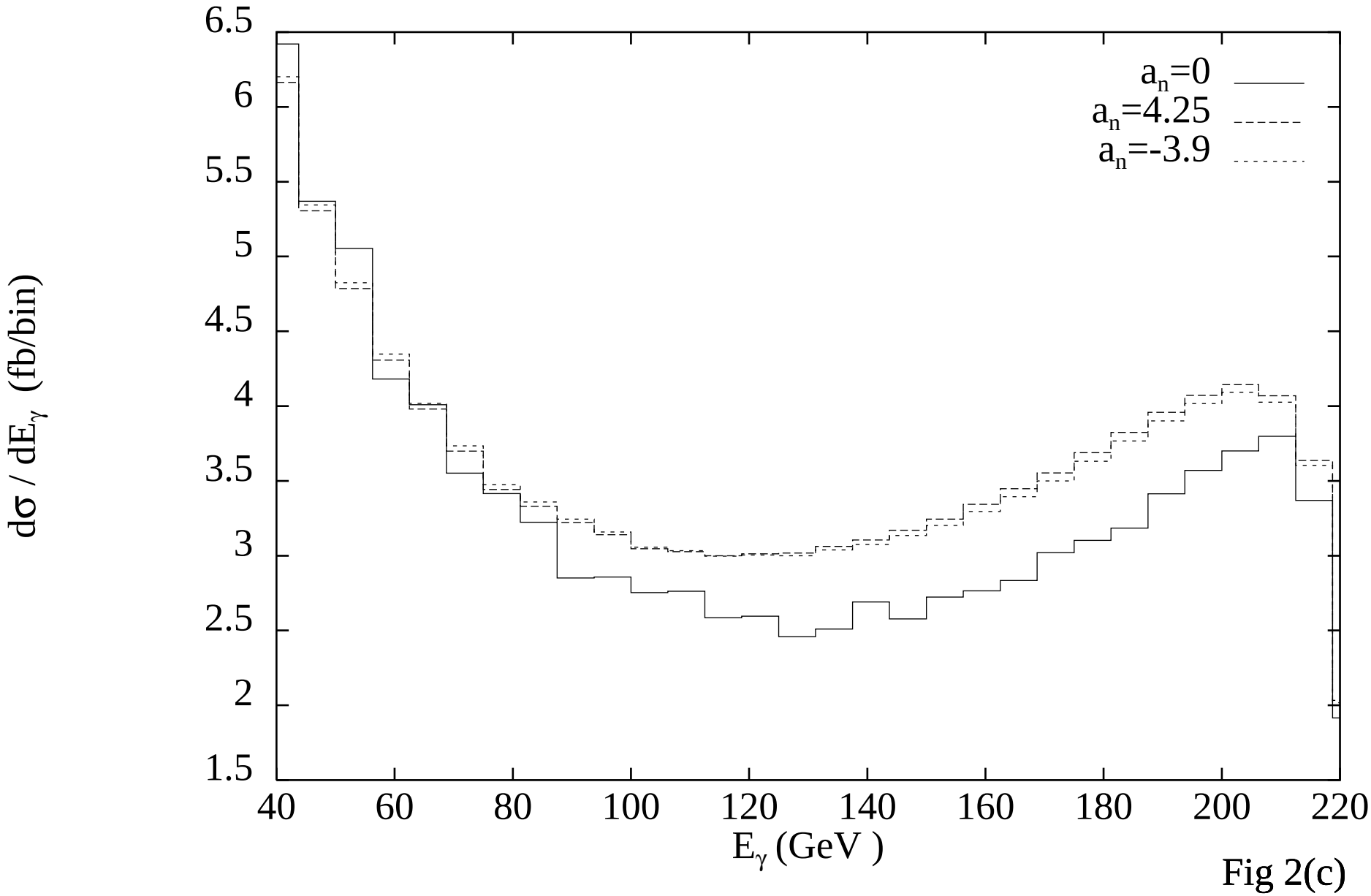
6.5
6
5.5
5
4.5
4
3.5
3
2.5
2
1.5
40
60
80
100
120
140
160
180
200
220
$d\sigma / dE_\gamma$ (fb/bin)
E_γ (GeV)
a_n=0
a_n=4.25
a_n=-3.9

Fig 2(c)

This figure "fig1-3.png" is available in "png" format from:

http://arXiv.org/ps/hep-ph/9406317v1

This figure "fig2-3.png" is available in "png" format from:

http://arXiv.org/ps/hep-ph/9406317v1

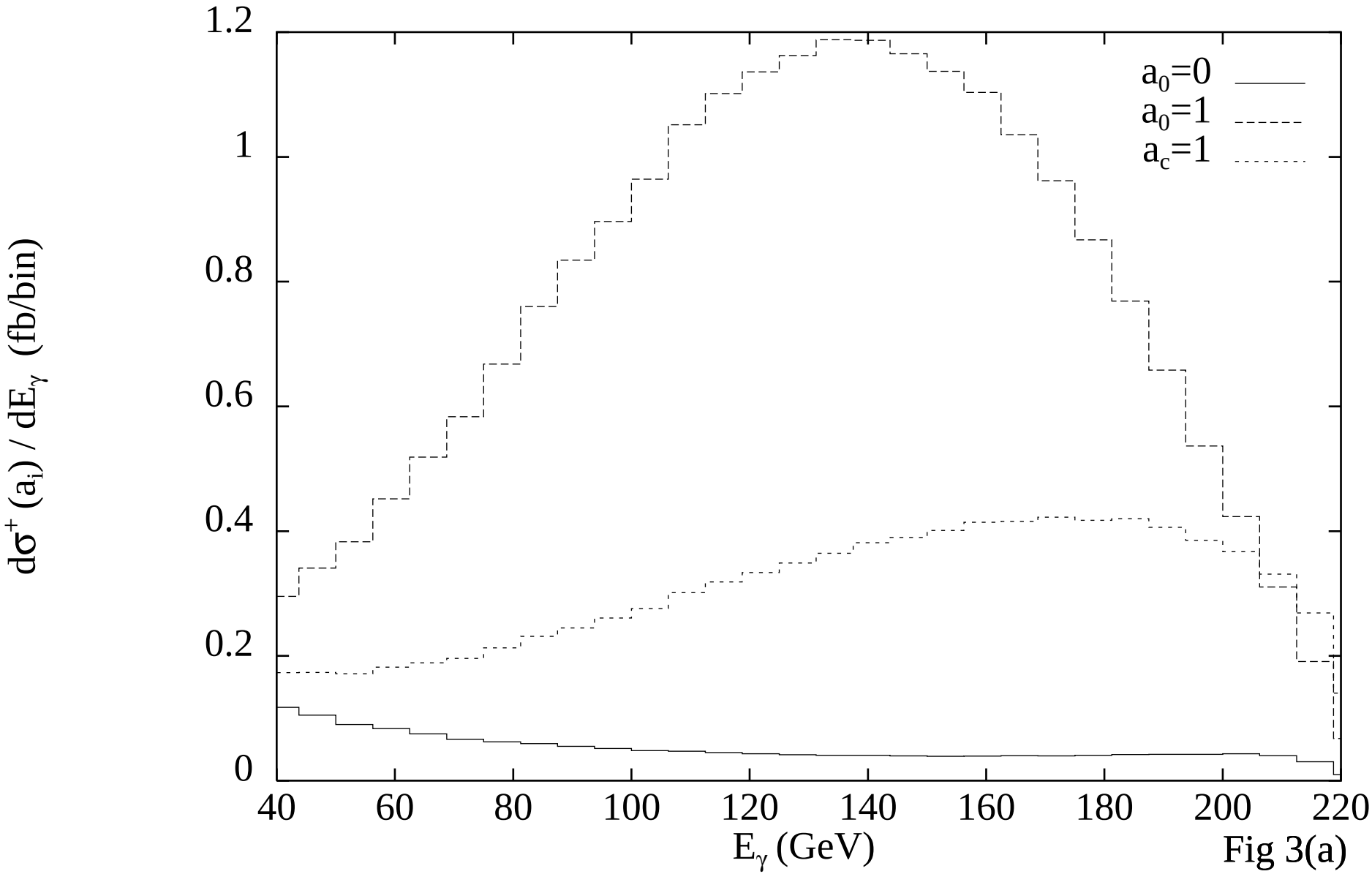
1.2
1
0.8
0.6
0.4
0.2
0
40
60
80
100
120
140
160
180
200
220
a_0=0
a_0=1
a_c=1
$d\sigma^+(a_i) / dE_\gamma$ (fb/bin)
E_γ (GeV)

Fig 3(a)

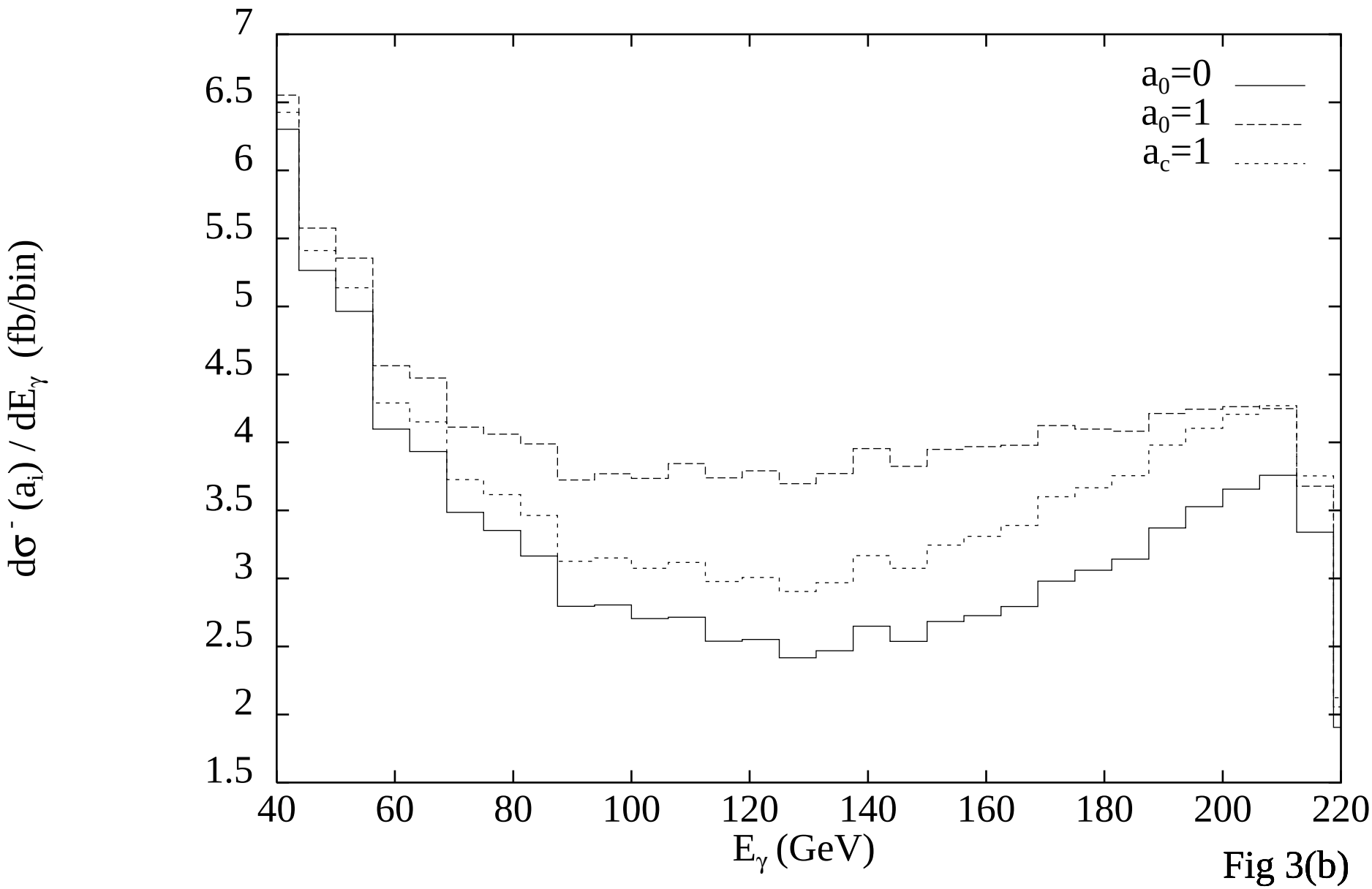
$d\sigma^-(a_i) / dE_\gamma$ (fb/bin)
7
6.5
6
5.5
5
4.5
4
3.5
3
2.5
2
1.5
40
60
80
100
120
140
160
180
200
220
E_γ (GeV)
a_0=0
a_0=1
a_c=1

Fig 3(b)

This figure "fig1-4.png" is available in "png" format from:

http://arXiv.org/ps/hep-ph/9406317v1

This figure "fig2-4.png" is available in "png" format from:

http://arXiv.org/ps/hep-ph/9406317v1

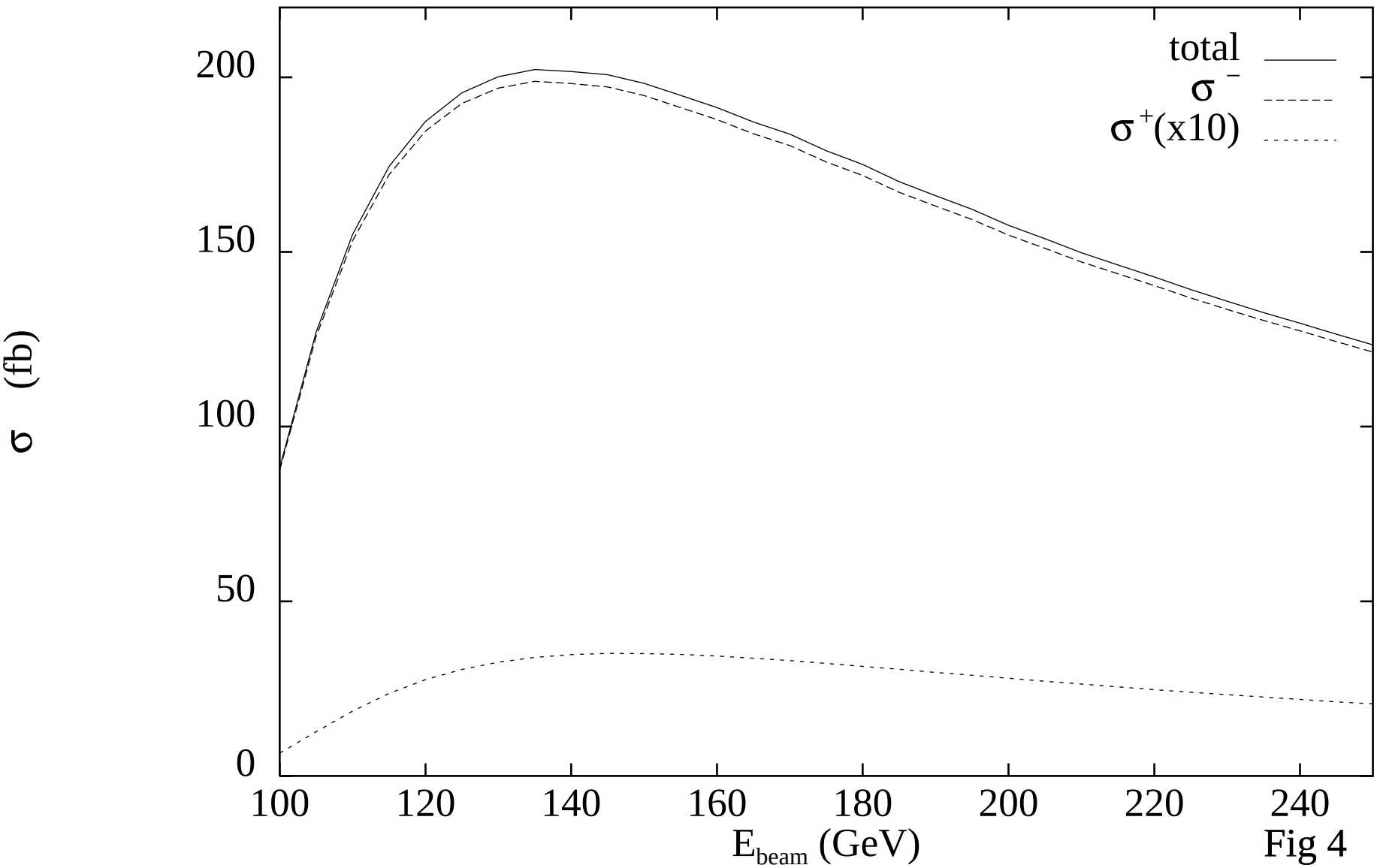
total
σ⁻
σ⁺(x10)
200
150
100
50
0
σ (fb)
100
120
140
160
180
200
220
240
E_beam (GeV)

Fig 4

This figure "fig2-5.png" is available in "png" format from:

http://arXiv.org/ps/hep-ph/9406317v1

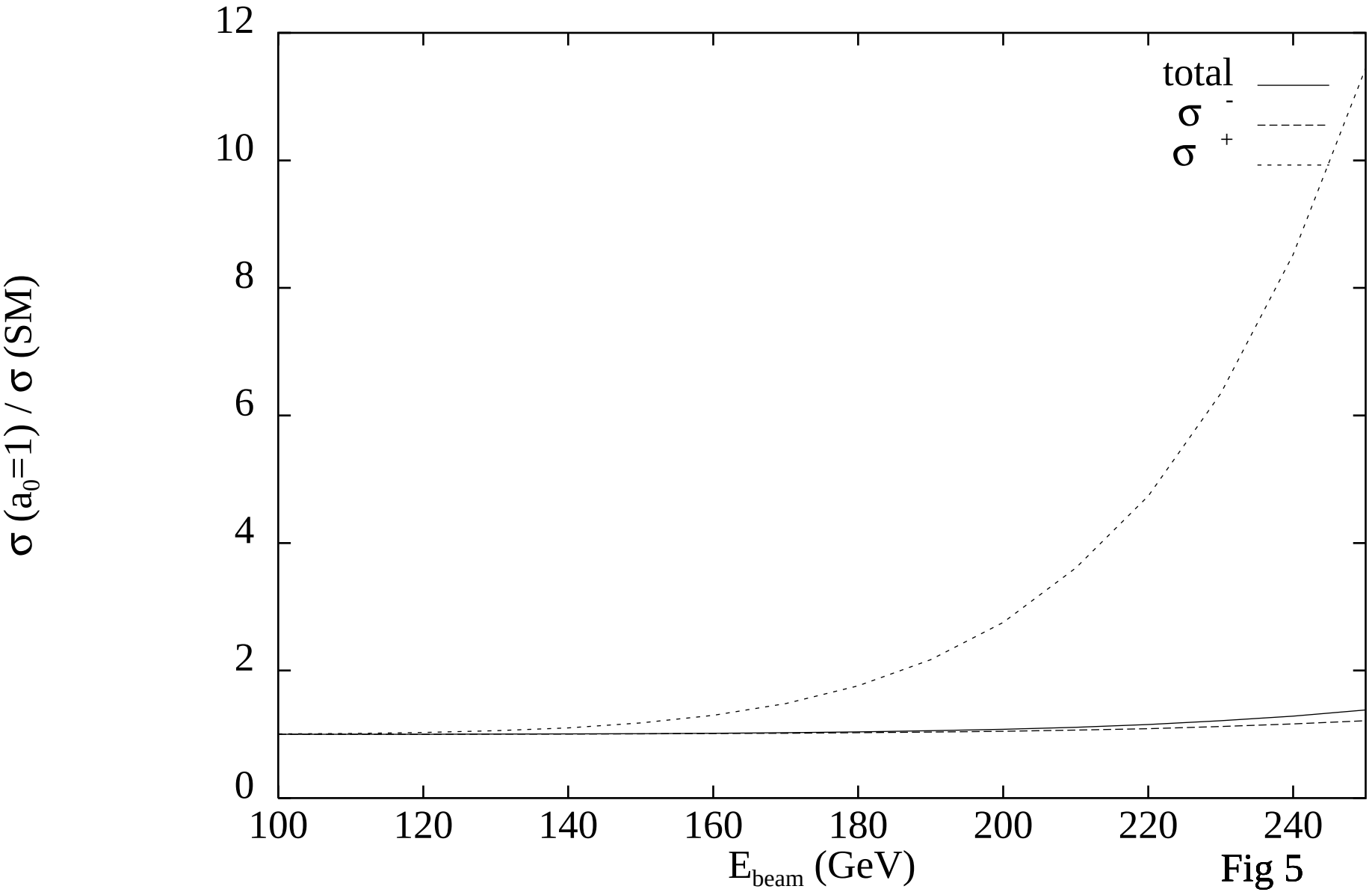
12
10
8
6
4
2
0
100
120
140
160
180
200
220
240
total
σ -
σ +
σ (a0=1) / σ (SM)
Ebeam (GeV)

Fig 5

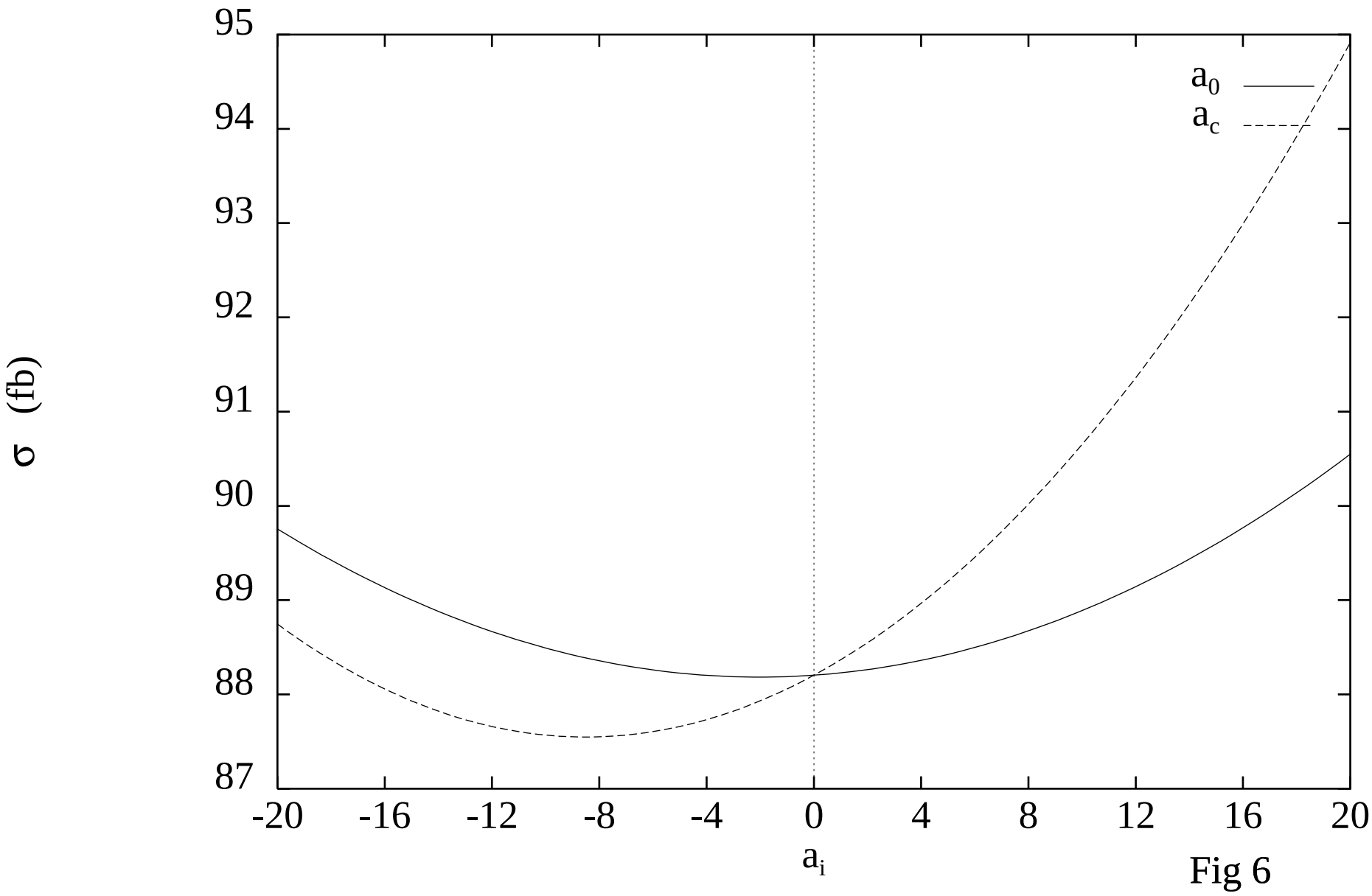

Fig 6